 doi:10.20944/preprints202205.0326.v1

Buckling behavior of different types of woven structures under axial compression loads

Guang-Kai Song[1] and Bo-Hua Sun*[1]

[1]School of Civil Engineering Institute of Mechanics and Technology
Xian University of Architecture and Technology, Xian 710055, China
*Corresponding author: B.H.S. email: sunbohua@xauat.edu.cn

Weaving is an ancient and effective structural forming technique characterized by the ability to convert two-dimensional ribbons to three-dimensional structures. However, most 3D structures woven from straight ribbons have topological defects. Baek et al.[15]proposed a method to weave smoother continuous 3D surface structures using naturally curved (in-plane) ribbons, obtained a new surface structure with relatively continuous variation of Gaussian curvature, and analyzed its geometric properties. We believe that this new 3D surface structure with smooth geometric properties must correspond to new mechanical properties. To this end, we investigated a 3D surface structure using naturally curved (in-plane) ribbon weaving, and the results of calculations and experiments show that such structures have better buckling stability than those woven with straight ribbons. It is observed that the number of ribbons influences the buckling behavior of different types of woven structures.

Keywords: In-plane curvatures, Buckling, Woven structure, 3D print, Gaussian curvature

I. INTRODUCTION

The design and manufacture of 3D structures has often been investigated [1-4]. These are manufactured by creating 2D planar structures and using methods such as driving [5-8], or processes such as folding, weaving, or inflating [9-11] to form 3D structures. You et al. [12] proposed a general method for the design of 2D foldable structures by extending and generalizing the standard trellis-type foldable structure consisting of two sets of parallel straight rods connected by hinges, which increases the range of shapes that can be achieved, and the boundary. Zhao et al. [13] introduced well-controlled twisting deformation to processes for mechanically driven geometric transformations of planar 2D structures to 3D architectures, enabling previously impossible features such as out-of-plane helical layouts. The method utilizes an elastomeric substrate with a shear pattern that deforms under strain, whose distribution can be designed precisely by computational methods. Lin et al. [14] exploited microscale features (e.g., plate thickness) enabled by two-photon direct laser writing to fabricate a variety of 3D origami metamaterials that display remarkable mechanical properties, underscored the scalable and multifunctional nature of origami designs, and paved the way toward harnessing the power of origami engineering at small scales.

How to form some curved 3D structures with continuous geometry using planar structures such as ribbons or rods has been a huge challenge. To solve this problem, Baek et al. [15] proposed a 3D surface forming method based on traditional weaving technology, containing ribbons with in-plane curvatures to weave, and using rivets to fix between ribbons. This method can realize a smoother and more continuous 3D surface structure, and its Gaussian curvature is closer to a continuum. The 3D structure woven by ribbons with in-plane curvatures has fewer geometric defects, and the rivets greatly increase the flexibility of the structure. Baek et al. [15] also deduced the formula of Gaussian curvature, laying a theoretical foundation for the formation of new woven structures. The formula for calculating the Gaussian curvature of a woven structure is shown below:

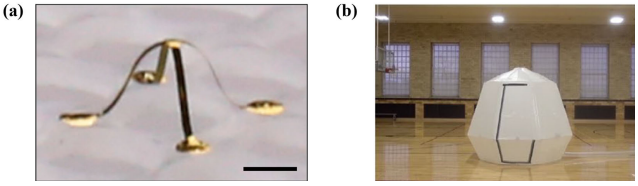

FIG. 1: 3D structure fabricated by planar structure: (a) 3D structure based on paper-cutting substrate driven by buckling [13]; (b) Inflatable folding structure [10].

$$K_n = \begin{cases} \frac{\pi}{3}(6-n), & \text{With straight ribbons;} \\ \frac{\pi}{3}[6-n(1+\kappa^*)], & \text{With curved ribbons.} \end{cases} \quad (1)$$

Where K_n is the Gaussian curvature of the woven structure, and n is the number of ribbons, κ^* is the in-plane curvature of ribbons. Based on this, Ren et al. [16] designed various structures using ribbons with in-plane curvatures. We can see that the weaving of ribbons with in-plane curvatures can solve the formation problem of 3D curved surface structures.

The geometric characteristics of a woven structure fabricated by ribbons with in-plane curvatures has been ana-

Preprints (www.preprints.org) | NOT PEER-REVIEWED | Posted: 24 May 2022 doi:10.20944/preprints202205.0326.v1

lyzed in the literature [15], but not the mechanical properties. In this paper, we combine 3D printing, experiments, and the finite element method (FEM) to analyze the axial buckling behavior of different types of woven structures. Compared with other woven structures, the structure with ribbons with in-plane curvatures not only has a smoother and more continuous geometric configuration, but a higher axial buckling load. Under the same number of ribbons, the new woven structure is more stable.

The rest of the paper is organized as follows. Structures woven by different types of ribbons are analyzed, and it is found that the new woven structure has a higher axial buckling load and better structural stability. We then study the hybrid woven structure and new woven structure, and analyze the influence of different numbers of ribbons on their axial buckling load. The forming method of a finite element model of a woven structure considering ribbon thickness and the driving of force displacement is proposed. The finite element buckling analysis of woven structures is carried out, and the correctness of the model is verified by experiments.

II. BUCKLING ANALYSIS OF DIFFERENT WOVEN STRUCTURES

A. Fabrication of different types of woven structures

We experimentally study the buckling behavior of woven structures. It can be seen [15] that woven structural ribbons adopt a straight ribbon or a ribbon with in-plane curvatures, and the structure consists completely of the same type of ribbon. On this basis, a hybrid weaving structure with naturally curved ribbons and a straight strip is proposed. To accurately obtain these three kinds of woven structures, we use 3D printing to obtain a single ribbon connected by rivets, using a ZRapid Tech SLA880 3D printer and R2024 plastic rivet model, as shown in Fig. 2.

After getting different types of ribbons, a single ribbon must be woven into a 3D structure, through the process shown in Fig. 3. A single ribbon is lapped into a plane shape, so that rivet holes 2 and 3 in different ribbons overlap each other. Plastic rivets are used to fix the overlapping rivet holes in the plane structure, and a stable plane structure is formed. As shown in Fig. 3(e), the ribbon of the plane structure is moved along the direction of the arrow, so that the two rivet holes overlap with each other, and are finally fixed with plastic rivets to form a 3D woven structure. It can be seen that the position between the rivet holes 1,4 and the point of intersection of the ribbon of the plane structure is an important factor in the formation of the 3D woven structure.

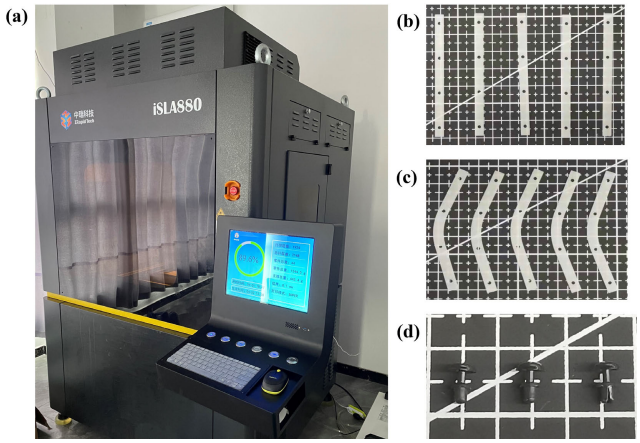

FIG. 2: 3D printing of different types of ribbons: (a) 3D printer; (b) Straight ribbons for 3D print; (c) Ribbons with in-plane curvatures for 3D print; (d) Physical drawing of rivets.

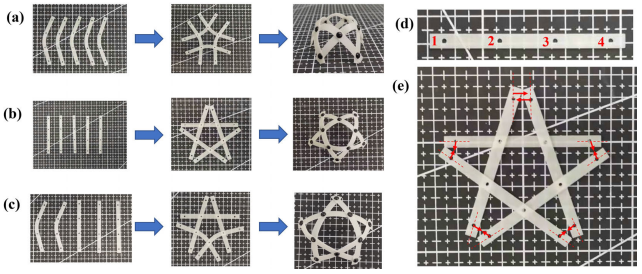

FIG. 3: Fabrication process of woven structure: (a) With naturally curved ribbons; (b) With straight ribbons; (c) Mixed woven structure with three straight ribbons and two naturally curved ribbons.

Fig. 4 shows the formation of woven structures with different Gaussian curvatures. From Fig. 4(b1), we can see that when the intersection point of the ribbon's axis is just the intersection point between the two rivet holes, only the plane structure can be obtained, and the 3D woven structure cannot be generated. When there is a certain distance between the two rivet holes, it is necessary to determine the position between the rivet holes and the intersection of the two ribbon axes. Assuming that the axis intersection appears inside the rivet hole, the 3D woven structure is negative Gaussian curvature, as shown in Fig. 4(c2). If the axis intersection occurs outside the rivet hole, the woven structure is a positive Gaussian curvature structure, as shown in Fig. 4(a2).

Preprints (www.preprints.org) | NOT PEER-REVIEWED | Posted: 24 May 2022 doi:10.20944/preprints202205.0326.v1

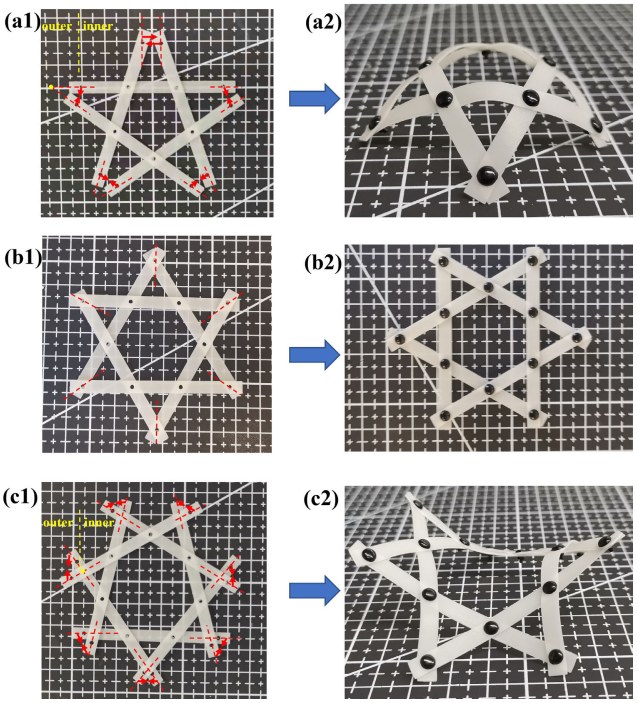

FIG. 4: Weaving structure with different Gaussian curvatures(K): (a2) $K > 0$; (b2) $K = 0$; (c2) $K < 0$.

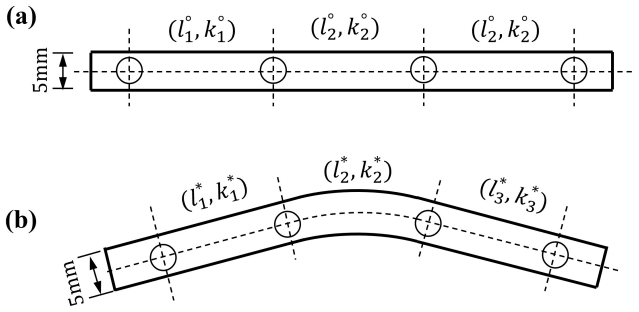

FIG. 5: Geometric size of ribbon, where l is arc length and k is curvature. $l_1^\circ = l_2^\circ = l_3^\circ = 20\ mm, k_1^\circ = k_2^\circ = k_3^\circ = 0, k_1^* = k_3^* = 0, k_2^* = -0.033\ mm^{-1}, l_1^* = l_2^* = l_3^* = 20\ mm$. Ribbon thickness is 0.5 mm.

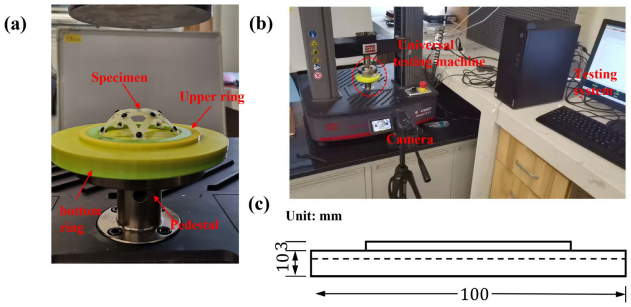

FIG. 6: Axial compression test platform.

B. Experimental Analysis of Different weaving Structures

The number of ribbons $n = 5$ was selected for this experiment, and axial compression tests were carried out on structures completely woven by straight ribbons (traditional woven structure), completely woven by ribbons with in-plane curvature (new woven structure), and woven by a mix of straight ribbons and ribbons with in-plane curvature (hybrid woven structure). The geometry of a single ribbon is shown in Fig. 5. To realize the boundary condition that the bottom of the 3D woven structure is fixed, a new bottom support was designed, which was divided into two parts, which were $3-mm$ and $10-mm$ circles. The specimen was first placed in the upper circles. Under axial pressure, the bottom of the specimen expanded outward along the radial direction. Due to the existence of the upper circles, the radial displacement of the structure was constrained to achieve a fixed boundary condition at the bottom. The lower part of the circles of the new support was connected with the bottom support of the universal testing machine, so that the new support could be fixed on the original support. The new bottom support was made by a thermal 3D printer, whose model is shown in Fig. 6.

Displacement control was used in the whole loading process of this test. Before the beginning of the test, the upper axial pressure head was adjusted to contact the specimen. To ensure the specimen could withstand a quasistatic axial pressure load, the downward pressure velocity of the upper axial pressure head was 1 mm/min. The axial load-displacement curves of different woven structures are shown in Fig. 7, from which it can be seen that the curves of the three woven structures show a trend of increasing, decreasing, and increasing again. In the case of the same number of ribbons, the woven structure with ribbon with in-plane curvatures has a higher buckling load capacity, and its initial stiffness is greater than with straight ribbons; this is because the woven structure fabricated by naturally curved ribbons has a relatively continuous geometric configuration, and the structure has good stiffness and stability. The initial stiffness and maximum axial load of the woven structure fabricated by mixing straight ribbon (3) and bending ribbon (2) are lower than those of the other two woven structures. Compared with the other two kinds of woven structures, the woven structure fabricated by straight ribbons reached the lowest point of axial pressure very early; meanwhile, the woven structure fabricated by naturally curved ribbons reached the lowest point of load late and had good deformation ability.

According to the deformation diagrams of different wo-

Preprints (www.preprints.org) | NOT PEER-REVIEWED | Posted: 24 May 2022 doi:10.20944/preprints202205.0326.v1

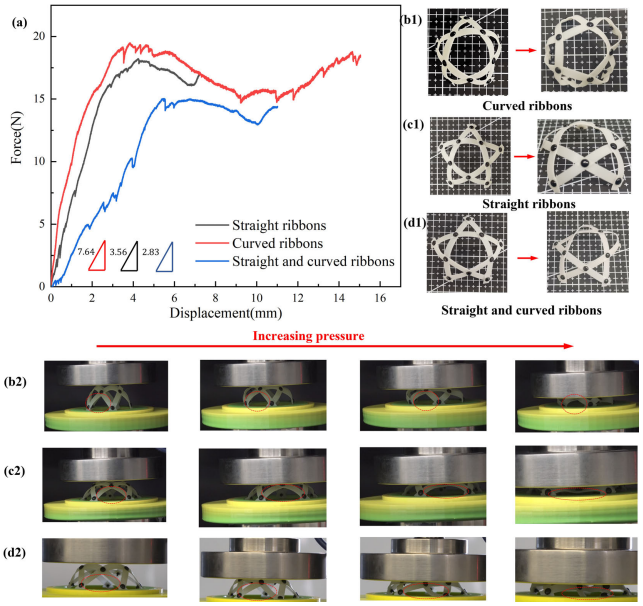

FIG. 7: Test curves and failure modes of different woven structures.

ven structures in Fig. 7, it can be seen that, compared with the woven structure fabricated by a single type of ribbon, the deformation of the hybrid ribbon woven structure is asymmetric, and there is symmetric deformation of other structures. At the late stage of loading, the deformation of the structure increases, the bottom rivet is in contact with the upper edge of the base, and the structure is transformed from a ribbon to the bottom plastic rivet bearing the upper pressure, resulting in a certain increase in the buckling bearing capacity of the structure at the late stage of loading. Through comparison, it is found that the deformation of the woven structure fabricated by straight ribbons is concentrated at the bottom node, and the deformation of a single ribbon is small, which is unfavorable to the structure. In the woven structure fabricated by naturally curved ribbons, the ribbons are destroyed first and the joints are deformed later. The ribbon becomes the main load-bearing element of the woven structure. From the above analysis, we find that the woven structure fabricated by naturally curved ribbons has both a relatively smooth and continuous geometry, and good stability.

III. INFLUENCE OF DIFFERENT NUMBERS OF RIBBONS ON BUCKLING BEHAVIOR OF WOVEN STRUCTURES

Through the above analysis, it is found that with the same number of ribbons, the 3D structure woven by different types of ribbons has different mechanical properties. To investigate the effect of different numbers of ribbons on the weave structure, we conducted experimental studies on the hybrid weave structure and the new weave structure fabricated by naturally curved ribbons. Furthermore, we investigated the effects of different numbers of ribbons on the buckling mechanical properties of woven structures.

A. Effect of Different Numbers of Ribbons on Mixed Weaving Structure

To study the influence of the number of straight ribbons in the hybrid woven structure on its buckling mechanical properties, four hybrid woven structures were designed according to the number of straight ribbons, $n_s = 1, 2, 3, 4$. The size of the ribbon is shown in Fig. 5. The fabrication process of the specimen ribbon was the same as described above. A diagram of the specimen and the axial load-displacement curve obtained from the test is shown in Fig. 8.

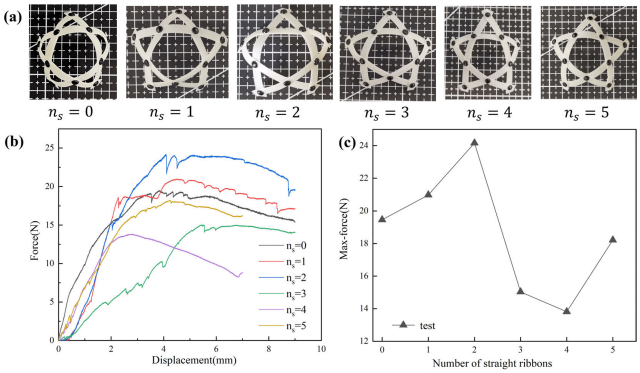

FIG. 8: Axial load-displacement curves of woven structures with different numbers of straight ribbons.

For convenience of comparison, the axial load-displacement curve obtained in Fig. 7 is placed in Fig. 8, where the woven structures formed entirely by straight ribbons and entirely by naturally curved ribbons are defined as $n_s = 5$ and $n_s = 0$, respectively. It can be seen from the figure that the woven structure has different degrees of buckling. When the number of straight ribbons is $n_s = 2$, the axial compression load of the hybrid woven structure reaches the maximum. With the increase of the number of straight ribbons, the buckling bearing capacity of the woven structure decreases. The axial compression load of the hybrid woven structure ($n_s = 0, 1, 2, 3, 4, 5$) increases, decreases, and then increases with the increase of the number of straight ribbons.

Fig. 9 is the failure mode diagram of different mixed woven structures. The failure mode of the structure when

Preprints (www.preprints.org) | NOT PEER-REVIEWED | Posted: 24 May 2022 doi:10.20944/preprints202205.0326.v1

$n_s = 0, 3, 5$ is introduced above, and is not mentioned here. For the woven structure at $n_s = 1, 2, 4$, according to Fig. 9, we can see that with the increase of displacement load, each structure has different degrees of buckling failure. When $n_s = 1$, the deformation of ribbon 1 (straight ribbon) in the hybrid woven structure is small, and the ribbons with in-plane curvature have irreversible deformation. Severe out-of-plane deformation occurs in ribbons 3 and 4, resulting in the bulge of connection points. Due to the deformation of the naturally curved ribbon, the external connection point of the structure is damaged to varying degrees, and the bending angle is 90°.

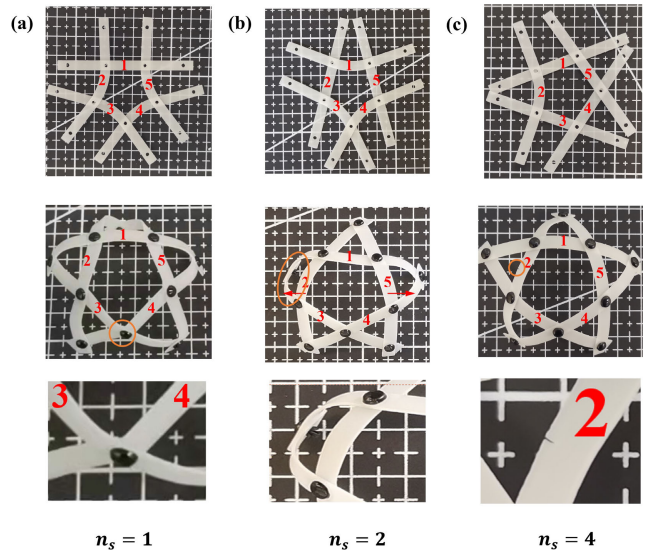

FIG. 9: Failure modes of woven structures with different numbers of straight ribbons.

When $n_s = 4$, only ribbon 2 (naturally curved) of the hybrid woven structure undergoes large in-plane deformation under axial load, and cracks occur in the middle segment of the ribbon. Fig. 9 shows that (b) is the failure mode when $n_s = 2$, and the 2, 5 (straight) ribbon does not undergo large deformation, but extends outward. The deformation of other ribbons is driven by the connection point. At the late loading stage, the deformation of members 1, 3, and 4 increased, and finally led to the deformation of structural support nodes. This is because of the step-by-step deformation that the hybrid woven structure has a higher axial buckling load.

Through the above analysis, it can be found that when the hybrid woven structure is subjected to an axial load, the deformation is mainly concentrated in the ribbons with in-plane curvatures, while the straight members do not have large deformation. When the woven structure fabricated entirely by naturally curved ribbon is subjected to vertical load, the ribbon with in-plane curvature first deforms, and then the bottom connection fails at the late loading stage. Because the woven structure composed of straight ribbons is not deformed, and the load is mainly concentrated at the bottom connection, the connection point is often destroyed, which is unfavorable to the whole structure. With 2 straight ribbons, a hybrid woven structure with high buckling load can be obtained by reasonably arranging the positions of straight and naturally curved ribbons.

B. Effect of Different Numbers of Ribbons on New Weaving Structure

To explore the influence of different numbers of ribbons on the axial compression load of a woven structure composed of naturally curved ribbons, structures of $n = 5, 6, 7$ ribbons were experimentally studied. The ribbon thickness of the woven structure was 0.5 mm, and the other geometric properties of ribbon are shown in Fig. 5. The test device of the specimen is shown in Fig. 6. The test loading was controlled by displacement, and the loading rate was 1 mm/min. The axial load-displacement curve obtained from the test is shown in the following figure.

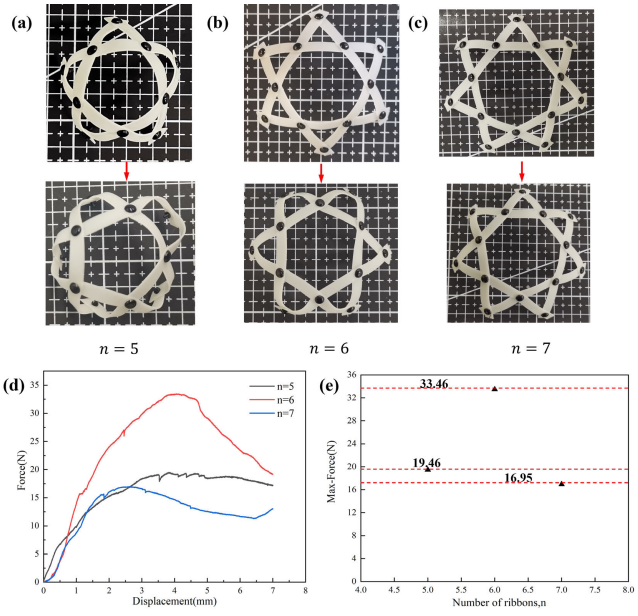

FIG. 10: Failure modes of woven structures with different numbers of ribbons with in-plane curvatures.

It can be seen from Fig. 10 that when the number of ribbons is 6, the woven structure has a high initial stiffness and axial compression buckling load, and its maximum axial compression buckling load is about twice that of the structure with $n = 7$ ribbons. We can see from the mode of failure that the regular polygon composed of in-

Preprints (www.preprints.org) | NOT PEER-REVIEWED | Posted: 24 May 2022 doi:10.20944/preprints202205.0326.v1

ternal nodes of the structure remains unchanged, and the deformation of the ribbon is mainly concentrated in the ribbon segment at the bottom connection point. As the number of ribbons increases, the deformation of the woven structure decreases gradually. With $n = 5$, a slight in-plane buckling of a single ribbon occurs. When the number of ribbons increases, this phenomenon gradually disappears, and only out-of-plane deformation occurs in the ribbons. This is because, as n increases, the curvature of the new woven structure decreases gradually, and the naturally curved ribbons are closer to the parallel bottom. Due to the constraint of rivets, the deformation degree of the ribbon structure decreases gradually under axial pressure, and mostly consists of out-of-plane bending.

Through the above analysis, it can be concluded that the number of ribbons with in-plane curvatures has a great influence on the buckling bearing capacity of the woven structure, and the appropriate number of ribbons can give it a greater initial stiffness and axial buckling load.

IV. FINITE ELEMENT ANALYSIS OF WEAVING STRUCTURE

To more comprehensively study the buckling mechanical properties of woven structures, ABAQUS was used to establish an accurate finite element model of the woven structure in combination with the above tests, using an elastic modulus of 1200 Mpa, density 1.12 g/cm^3, and Poisson's ratio 0.44. Because the woven structure is a 3D structure fabricated by 2D ribbons, its forming process is particularly important, so finite element models were established for the formation and buckling analysis of the woven structure.

A. Forming of woven structure in finite element method

A method to form a finite element model of weaving structure forming has been proposed in the literature [15], considering only the final shape of the structure, and not the effect of the thickness of individual ribbons. This makes ribbons intersect each other, and does not well simulate the actual woven structure. We propose a finite element woven structure forming model considering a single ribbon thickness driven by force and displacement.

In this paper, a 3D deformed shell is used to create a single ribbon of thickness is 0.5 mm, whose geometric size is shown in Fig. 5. The created ribbons are arranged in a flat shape as required, and a distance of 0.5 mm is left between the ribbons to ensure that they overlap. Simulation of weaving structure forming using quasistatic in dynamic implicit analysis step. The contact part adopts the general contact, the friction is defined in the tangential direction, and the friction coefficient is 0.3, which is vertically defined as hard contact. To simulate the connection of rivets, the center of each rivet hole is set as a reference point, to which a rivet hole with internal overlap is coupled. After the constraints are determined, the force-displacement driving method is used to form the woven structure. It can be seen from Fig. 11(b) that the vertical force is first applied to the internal segment of ribbon, and the relative displacement load is applied to the rivet hole of the external segment of ribbon, so that the two rivet holes overlap each other. To speed up the calculation and eliminate the self-locking of mesh shearing, the shell element S4R is used. The mesh size of woven structure is 0.2mm. The final simulation results are shown in Fig. 12.

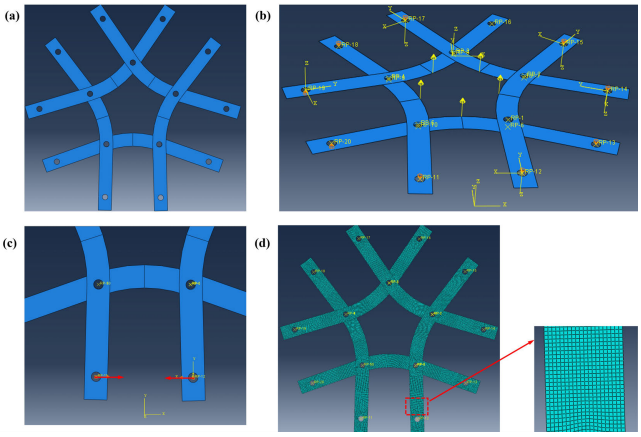

FIG. 11: Finite Element Model of Weaving Structure.

As can be seen in Fig. 12, the inner ribbon segments of the planar structure shift upward under the vertical force. Immediately afterward, the rivet holes on the outside of the structure approach each other, while at the same time the upper disturbance force is withdrawn. The structure continues to move upward as a whole due to the displacement of the bottom strip, eventually forming a 3D woven structure. The plastic rivet is not modeled in the finite element, but rather the top and bottom rivet holes are connected together by in-plane coupling. The woven structure generated by the finite element model is found to be similar to the actual woven structure.

Preprints (www.preprints.org) | NOT PEER-REVIEWED | Posted: 24 May 2022 doi:10.20944/preprints202205.0326.v1

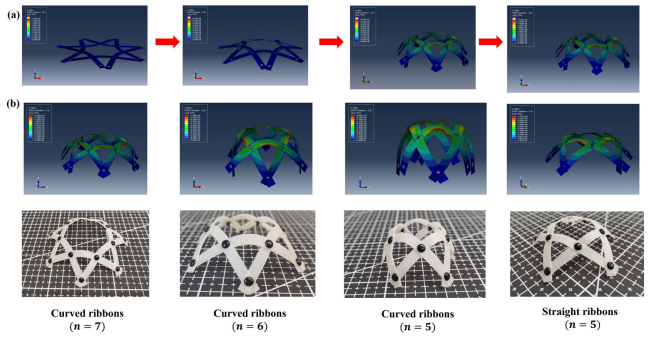

FIG. 12: Comparison between finite element models and actual models

B. Finite Element Simulation of 3D woven Structure

After obtaining the finite element model of the above weaving structure, the results are imported into the finite element again in the form of parts. Since the imported component is the computed model, structures are given mesh properties. To eliminate the mesh, we generate a new geometry, using a geometric editing function to re-edit the import model. After the finite element model is obtained, the material properties are given to the structure, with the same material parameters as woven molding. To fully restore the test, we establish a rigid plate in the finite element simulation to simulate the upper pressure head of a universal testing machine, which applies vertical displacement. Dynamic implicit quasistatic analysis is used in the simulation analysis. The displacement load is applied, and the loading rate is controlled at 1 mm/min. The element type is shell element S4R. The finite element model and mesh distribution are shown in Fig. 13.

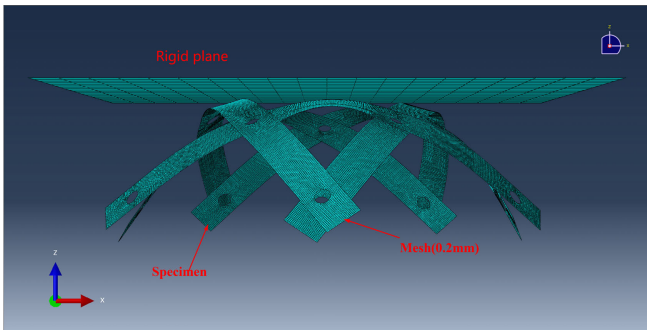

FIG. 13: Finite element mesh distribution. The mesh size of rigid plate is 5 mm. The mesh size of woven structure is 0.2 mm

In this section, the ABAQUS modeling of woven structure using the above method and finite element simulation of the different woven structures is presented. To confirm the above modeling method and the finite element model, with $n = 5$ ribbons, the 3D structure woven by straight ribbons is used for simulation, whose results are compared with the test results, as shown in Fig. 14.

From Fig. 14(a), we can see that the initial stiffness of the finite element simulation results is in good agreement with the test, but the maximum axial buckling load from the simulation is slightly higher than that of the test. Because the coupling approach is used in the finite element simulation to simulate the plastic rivet, but in practice there is a certain gap between the rivet and the rivet hole, compared to the coupling in the finite element, its constraint strength is weaker. In addition, the complete restraint on the bottom of the specimen leads to a higher overall restraint strength of the finite element model, which, together with some unavoidable errors and initial defects in the test, leads to a slightly higher axial compression load in the finite element simulation than the test value.

From the failure mode diagram of the test, it can be seen that the finite element can simulate the ribbon bending of the woven structure in the test, and the overall failure mode of the structure is similar to that of the test. The above analysis shows that the finite element method of using force-displacement-driven weaving structure forming is well suited to the actual weaving structure, and solves the problem of model crossing without considering member thickness in finite elements. The above finite element model of force-displacement driving molding is used for simulation to solve the problem of the difficult modeling of the woven structure. Compared with the test, it is found that this method can more accurately simulate the axially compressed mechanical properties of woven structures in practice.

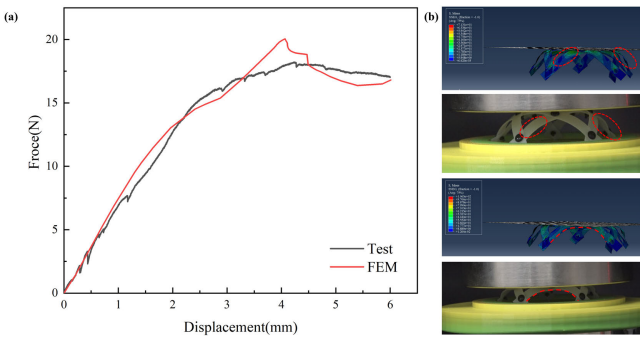

FIG. 14: Verification of finite element model of woven structure: (a) Comparison of axial load-displacement curves; (b) Comparison of failure modes.

V. CONCLUSION

We studied the buckling behavior of different woven structures by combining experimental and finite element methods. It was demonstrated that, compared with the traditional woven structure, the new woven structure with in-plane bending ribbons has higher initial stiffness and a larger axial buckling load. In addition, we investigated the effect of different numbers of ribbons on the buckling behavior of the new woven structure and a hybrid woven structure. It was shown that the axial buckling load of the hybrid woven structure is greatest when the number of straight ribbons is 2. With the increase of the number of straight ribbons, the buckling load of the hybrid woven structure decreases, and then increases. By contrast, the axial buckling load of the new woven structure reaches the maximum when the number of ribbons is 6. To address the problem that finite element models in the literature [15] have different ribbons crossing each other, we formed a finite element weaving structure driven by force-displacement while considering the ribbon thickness. A finite element buckling analysis was then performed on the molded woven structure. The axial obtained load-displacement curve was in good agreement with the experimental data, indicating that this model can accurately simulate the buckling mechanical properties of the weaving structure.

[1] T. Nakamoto, K. Yamaguchi, P. A. Abraha, K. Mishima, Manufacturing of three-dimensional micro-parts by uv laser induced polymerization, Journal of micromechanics and microengineering 6(2) (1996) 240.

[2] Y. Zhang, F. Zhang, Z. Yan, Q. Ma, X. Li, Y. Huang, J. A. Rogers, Printing, folding and assembly methods for forming 3d mesostructures in advanced materials, Nature Reviews Materials 2 (4) (2017) 1-17.

[3] G. Huang, Y. Mei, Assembly and self-assembly of nanomembrane materialsfrom 2d to 3d, Small 14 (14) (2018) 1703665.

[4] J. Rogers, Y. Huang, O. G. Schmidt, D. H. Gracias, Origami mems and nems, Mrs Bulletin 41 (2) (2016) 123-129.

[5] S. Xu, Z. Yan, K. I. Jang, W. Huang, H. Fu, J. Kim, Z. Wei, M. Flavin, J. McCracken, R. Wang, A. Badea, Y. Liu, D. Xiao, G. Zhou, J. Lee, H. U. Chung, H. Cheng, W. Ren, A. Banks, X. Li, U. Paik, R. G. Nuzzo, Y. Huang, Y. Zhang, J. A. Rogers, Assembly of micro/nanomaterials into complex, three-dimensional architectures by compressive buckling, Science 347 (6218) (2015) 154-159.

[6] Y. Ling, X. Zhuang, Z. Xu, Y. Xie, X. Zhu, Y. Xu, B. Sun, J. Lin, Y. Zhang, Z. Yan, Mechanically assembled, three-dimensional hierarchical structures of cellular graphene with programmed geometries and outstanding electromechanical properties, ACS nano 12 (12) (2018) 12456-12463.

[7] W. Lee, Y. Liu, Y. Lee, B. K. Sharma, S. M. Shinde, S. D. Kim, K. Nan, Z. Yan, M. Han, Y. Huang, Y. Zhang, J. H. Ahn, J. A. Rogers, Two-dimensional materials in functional three-dimensional architectures with applications in photodetection and imaging, Nature communications 9 (1) (2018) 1-9.

[8] Y. Zhang, Z. Yan, K. Nan, D. Xiao, Y. Liu, H. Luan, H. Fu, X. Wang, Q. Yang, J. Wang, W. Ren, H. Si, F. Liu, L. Yang, H. Li, J. Wang, X. Guo, H. Luo, L. Wang, Y. Huang, J. A. Rogers, A mechanically driven form of kirigami as a route to 3d mesostructures in micro/nanomembranes, Proceedings of the National Academy of Sciences 112 (38) (2015) 11757-11764.

[9] M. Bern, B. Hayes, The complexity of at origami, in: SODA, Vol. 96, 1996, pp. 175-183.

[10] D. Melancon, B. Gorissen, C. J. García-Mora, C. Hoberman, K. Bertoldi, Multistable inatable origami structures at the metre scale, Nature 592 (7855) (2021) 545-550.

[11] B. Wang, G. Fang, H. Wang, J. Liang, F. Dai, S. Meng, Uncertainty modelling and multiscale simulation of woven composite twisted structure, Composites Science and Technology 217 (2022) 109118.

[12] Z. You, S. Pellegrino, Foldable bar structures, International Journal of Solids and Structures 34 (15) (1997) 1825-1847.

[13] H. Zhao, K. Li, M. Han, F. Zhu, A. Vzquez-Guardado, P. Guo, Z. Xie, Y. Park, L. Chen, X. Wang, H. Luan, Y. Yang, H. Wang, C. Liang, Y. Xue, R. D. Schaller, D. Chanda, Y. Huang, Y. Zhang, J. A. Rogers, Buckling and twisting of advanced materials into morphable 3d mesostructures, Proceedings of the National Academy of Sciences 116 (27) (2019) 13239-13248.

[14] Z. Lin, L. S. Novelino, H. Wei, N. A. Alderete, G. H. Paulino, H. D. Espinosa, S. Krishnaswamy, Folding at the microscale: Enabling multifunctional 3d origami-architected metamaterials, Small 16 (35) (2020) 2002229.

[15] C. Baek, A. G. Martin, S. Poincloux, T. Chen, P. M. Reis, Smooth triaxial weaving with naturally curved ribbons, Physical Review Letters 127 (10) (2021) 104301.

[16] Y. Ren, J. Panetta, T. Chen, F. Isvoranu, S. Poincloux, C. Brandt, A. Martin, M. Pauly, 3d weaving with curved ribbons, ACM Transactions on Graphics (TOG) 40 (4) (2021) 1-15.